

Nuclear Spin-Lattice Relaxation in Pure and Impure Indium. II. Superconducting State*

J. D. Williamson[†] and D. E. MacLaughlin

Department of Physics, University of California, Riverside, California 92502

(Received 18 December 1972)

Nuclear spin-lattice relaxation times $T_1(T)$ have been measured in superconducting indium and the $InGa$, $InCd$, $InTl$, $InHg$, and $InPb$ dilute-alloy systems, using a transient nuclear-quadrupole-resonance spectrometer. Local sample heating was identified and its effects minimized. No effects attributable to trapped flux were observed. For fixed T_c/T , T_1 decreases with increasing impurity concentration, which indicates that the anisotropy of the energy gap decreases with decreasing mean free path l . Although the effects of a mean-square anisotropy $\langle a^2 \rangle = 0.005 \pm 0.001$ are essentially averaged out for $l \lesssim \xi_0$ (the pair dimension), the data indicate additional gap broadening in the more concentrated alloys. Lifetime effects associated with thermal-phonon scattering of the quasiparticles are insufficient to explain the data, and we tentatively attribute the additional temperature- and solute-independent broadening to a 2% rms energy-gap inhomogeneity. Similar behavior is noted in previous measurements to T_1 in aluminum alloys. We find $\langle a^2 \rangle = 0.003 \pm 0.001$ for pure aluminum and suggest that an energy-gap inhomogeneity of about 1% rms determines the density of excited states in concentrated aluminum alloys.

I. INTRODUCTION

It has become clear in the past few years that the singularity in the superconducting density of excited quasiparticle states predicted by the BCS theory¹ is broadened in real superconductors by a number of mechanisms. It was recognized in analysis of early experimental data,²⁻⁵ and confirmed in later investigations,⁶ that the manner in which the BCS singularity is removed can be studied in some detail by measurement of nuclear spin-lattice relaxation (SLR) times in type-I superconductors. In the absence of pair-breaking processes (which will not be discussed further in this article), the principal mechanisms which can contribute to gap broadening appear to be energy-gap anisotropy (EGA), quasiparticle damping by thermally excited phonons (QPD), and energy-gap inhomogeneity (EGI); the importance of the latter mechanism in In and Al is suggested (but not proved) by the present results. Gap broadening always increases $T_1(T)$.²

Gap anisotropies of $\pm 20\%$ of the average gap value have been observed by single-crystal tunneling in tin,⁷ and the presence of anisotropy in the gap has been inferred in indium and other type-I superconductors from thin-film tunneling,⁸ ultrasonic attenuation, and thermal-conductivity measurements.⁹ Further evidence for EGA was obtained from the SLR measurements of Masuda¹⁰ in dilute aluminum-based alloys. According to Anderson's theory of dirty superconductors,¹¹ scattering from nonmagnetic impurities reduces the effect of anisotropy, but does not greatly affect other superconducting properties. In fact a dirty superconductor is often described by the BCS theory more accurately than the pure metal. Thus the SLR be-

havior corresponding to the BCS model should be recovered in the dirty limit. Masuda¹⁰ observed a decrease in the SLR time in aluminum as the mean free path was reduced, although the minimum in $T_1(T)$ corresponding to a BCS superconductor was not obtained for the most impure alloys investigated.

At about the same time, Fibich¹² showed that the finite lifetime of the quasiparticle excited states, due to scattering by thermal phonons, broadens the BCS singularity and thus increases $T_1(T)$. The importance of this broadening mechanism depends upon the strength of the dynamic electron-phonon coupling. For this reason quasiparticle damping (QPD) is calculated from the Eliashberg equations¹³ and is often referred to as a strong-coupling effect.

Recently, Larkin and Ovchinnikov¹⁴ have calculated the broadening of the density of states due to inhomogeneities of the effective interaction between electrons in superconductors. If the characteristic inhomogeneity dimension r_c is large compared with the pair dimension ξ_0 , then the density of states at each point has a local BCS character, and one recovers the BCS result for $T_1(T)$. However, if $r_c \ll \xi_0$, the density of states is broadened by an amount determined by the number, strength, and dimension of the inhomogeneities, and a $T_1(T)$ greater than the BCS value is also obtained.

This article reports a study of the dependence of $T_1(T)$ on both temperature and the concentration of nonmagnetic impurities in indium and its alloys. Evidence has been found for the presence of EGA, QPD, and a residual broadening which we tentatively attribute to EGI, on the basis of the following considerations: EGA should be essentially washed

out in the more concentrated alloys (≈ 1.0 at. %), whereas the electron-phonon interaction should not be appreciably affected by the solute concentration. (As will be seen below, in indium the residual contribution also appears to be independent of solute concentration.) In the dirty alloys, the relative importance of QPD and EGI can in principle be determined by the observed temperature dependence of $T_1(T)$. While EGI is presumably temperature independent, the contribution of QPD should decrease with temperature as the number of thermal phonons decreases. Thus the temperature dependence of $T_1(T)$ should in turn reflect the temperature dependence of the gap broadening, and thereby permit a determination of the broadening mechanism. Experimentally, the QPD model provided insufficient broadening and an incorrect temperature dependence to fit $T_1(T)$ results in dirty indium alloys.¹⁵ (In pure indium, EGA apparently dominates all other mechanisms.) However, it was possible to fit the data for dirty alloys equally well with curves based on both the "QPD + EGI" and the "EGI alone" picture. Thus a simple test based on temperature dependence proved to be insufficiently sensitive, and the choice of the "QPD + EGI" model was based on the values of a parameter involved in the fits, as described in Sec. VB.

SLR measurements have been made in the superconducting state of In, InGa, InCd, InTl, InPb, and InHg dilute (0.1–3.0-at. %) alloy systems. Section II describes the experimental procedure, and in Sec. III the SLR times are calculated for the three models discussed above. Section IV gives our results which are discussed in Sec. V together with those of Masuda¹⁰ in aluminum and Al alloys. Our conclusions are presented in Sec. VI. A preliminary report of part of this work has appeared elsewhere.¹⁵

II. EXPERIMENTAL

A. Samples

The In, InGa, InCd, InTl, and InPb samples used in this work have been described by Anderson *et al.*¹⁶ and Thatcher and Hewitt.¹⁷ A verification of the impurity concentrations of the alloys was made by measuring the superconducting transition temperatures. The results agreed with previous measurements of alloys with similar impurity concentrations.¹⁸

B. SLR Measurements

The nuclear-quadrupole-resonance (NQR) method described previously^{19,20} was used to measure the SLR times. A field-cycling technique was used to obtain signals below T_c .⁶ The difference signal between the echo amplitude $S_{9/2}(t)$ a time t after the initial saturating pulse, and a reference signal $S_{9/2}(t \rightarrow \infty)$, was recorded for the $|\frac{3}{2} | - | \frac{1}{2} |$ NQR tran-

sition. This difference signal $V_{9/2}(t) = S_{9/2}(t) - S_{9/2}(\infty)$ is proportional to the population difference¹⁹

$$u_{9/2}(t) = u_{9/2}(0) [0.121e^{-3t/T_1} + 0.559e^{-10t/T_1} + 0.297e^{-21t/T_1} + 0.022e^{-36t/T_1}]. \quad (1)$$

We write

$$V_{9/2}(t) = V_0 + (V_1 - V_0)u_{9/2}(t) \quad (2)$$

to account for the unknown system gain and baseline voltage V_0 . Here V_0 is the equilibrium signal for $t \gg T_1$, and V_1 is the signal extrapolated to $t = 0$. Data were taken for discrete times t_m , and V_0 , V_1 , and T_1 were varied for the best fit of the data set $\{V_{9/2}(t_m), t_m\}$ to Eq. (2).

C. Transient Heating

Transient sample heating was observed for temperatures below about 2 K. The data sets $\{V_{9/2}(t_m), t_m\}$ which included data for short times had unusually poor least-squares fits to the multiexponential relaxation function Eq. (2). We conclude that a portion of these data sets was taken during the time τ_{eq} required for thermal equilibrium to be established between the sample and the He⁴ bath after rf eddy-current heating by the initial saturating pulse. Unless thermal equilibrium exists the relaxation will not be described by a time-independent T_1 in the multiexponential expression Eq. (2).

The time τ_{eq} was determined experimentally by progressively eliminating from the data set the points for the initial observation times and examining both the average square residual in the least-squares fit and the best-fit value of T_1 . The average square residual decreased and T_1 increased to nearly stationary values at essentially the same value of the initial time t_i , which we have denoted as τ_{eq} . Figure 1 gives the best fit T_1 as a function of t_i for In + 0.8-at. % Tl. Extrapolations of the stationary values of T_1 to long t_i are shown, and an approximate locus $t_i = \tau_{eq}$ is given by the dashed line. Figure 2 shows the results of this correction procedure. The low-temperature curvature suggested by the uncorrected data and discussed previously⁶ is apparently a result of transient heating alone.

When this source of systematic error was eliminated, the 90% confidence level for V_0 and V_1 as obtained from the fitting program varied between ± 0.5 and $\pm 1.0\%$ and that for T_1 between ± 1 and $\pm 2\%$. The observed scatter of the T_1 values is more nearly $\pm 5\%$, especially at lower temperatures. This points to an additional source of random error, possibly associated with the extrapolation procedure, which does not appreciably affect our conclusions.

D. Cryogenics

He⁴ vapor-pressure thermometry and the T_{58} vapor-pressure temperature scale were used to cali-

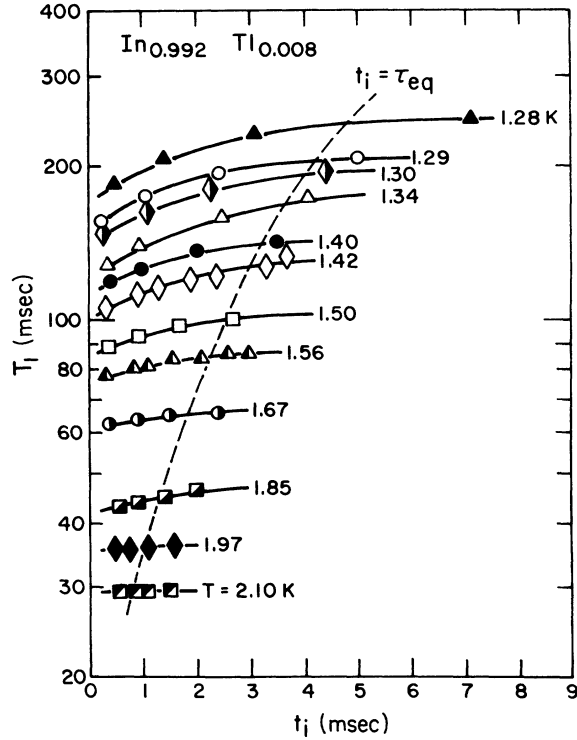


FIG. 1. Best-fit value of T_1 as a function of the initial observation time t_i . The time for thermal equilibrium τ_{eq} is defined by the condition $T_1 \approx \text{const}$ for $t_i > \tau_{eq}$.

brate a germanium resistance thermometer. The calibration accuracy is ± 0.002 K over the He⁴ range. The absence of appreciable *average* rf eddy-current heating at all temperatures was confirmed by varying the rf-pulse repetition rate and noting no change of the average sample temperature.

E. Trapped Flux

The presence of regions of trapped flux in SLR measurements would constitute a source of systematic error, since nuclei in the trapped field $H > H_c$ would presumably exhibit SLR behavior appropriate to the normal state.^{2,4} Although such a source of error cannot be ruled out, internal evidence points to its negligibility. First, the presence of normal and superconducting regions would lead to more than one T_1 , and thus to a degradation of the fit to Eq. (2) in the superconducting state. Apart from transient heating effects as discussed above, no such degradation was observed. Second, *any* presence of normal-state SLR should result in a reduction of the observed T_1 at low temperatures where $T_{ln} \ll T_{ls}$. This reduction would be expected to modify the exponential behavior of T_1 on inverse temperature in a manner which

again was not observed. We conclude that no evidence for trapped flux is found in the present SLR measurements.

III. THEORY

The nuclear SLR time in the superconducting state can be calculated from the usual golden rule formula for the transition rate; the result² is

$$T_{ln}/T_{ls} = (k_B T)^{-1} \int_{-\infty}^{\infty} n(\omega_i) n(\omega_f) C(\omega_i, \omega_f) \times f(\omega_i) [1 - f(\omega_f)] d\omega_i, \quad (3)$$

where k_B is the Boltzmann constant, $\omega_f = \omega_i + \text{nuclear Zeeman energy}$, $f(\omega)$ is the Fermi-Dirac distribution function, and T_{ln} is the normal-state relaxation time. $C(\omega_i, \omega_f)$ is the coherence factor,⁹ and $n(\omega)$ is the reduced quasiparticle density of states, which for a BCS superconductor is given by

$$n_{BCS}(\omega) = \text{Re} \{ [\omega^2 - \Delta_0^2(T)]^{-1/2} \}. \quad (4)$$

Here $\Delta_0(T)$ is the BCS gap parameter. For the BCS density of states, the integral in Eq. (3) diverges logarithmically for $\omega_f = \omega_i$. The divergence is removed by the small Zeeman splitting of the nuclear levels, but the unmodified BCS theory still yields

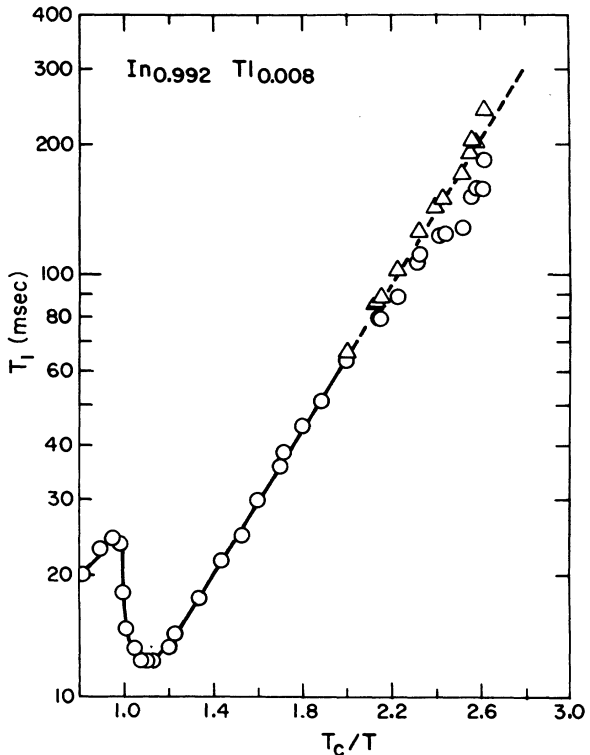


FIG. 2. Best-fit values of T_1 before (circles) and after (triangles) corrections for transient heating have been made.

a relaxation rate an order of magnitude larger than that observed experimentally. In a real superconductor any mechanism which redistributes or broadens the excited states near the gap edge will smear the density of states and tend to lengthen the relaxation times. Thus measurements of $T_1(T)$ can be used to examine the nature of the broadening mechanisms.

A. Energy-Gap Anisotropy

Clem²¹ developed a theory for anisotropy by assuming a separable potential for the pairing interaction:

$$V_{\vec{p}, \vec{p}'} = [1 + a(\vec{\Omega})] V [1 + a(\vec{\Omega}')] \quad (5)$$

The anisotropy function $a(\vec{\Omega})$ is given by

$$a(\vec{\Omega}) = [\Delta(T, \vec{\Omega}) - \langle \Delta(T, \vec{\Omega}) \rangle] / \langle \Delta(T, \vec{\Omega}) \rangle, \quad (6)$$

where $\Delta(T, \vec{\Omega})$ is the energy gap at temperature T as a function of direction $\vec{\Omega} = \vec{p}/|p|$ on the Fermi surface. $\langle \Delta(T, \vec{\Omega}) \rangle$ is the average gap in a pure single crystal. The precise distribution of $a(\vec{\Omega})$ on the Fermi surface is generally unknown, so that an assumed anisotropy distribution function $P(a)$ is introduced. $P(a) da$ gives the fraction of the Fermi surface for which $a(\vec{\Omega})$ lies between a and $a + da$. The Fermi surface average is then defined to be

$$\langle F[\Delta(T, \vec{\Omega})] \rangle = \int da P(a) F[\langle \Delta(T, \vec{\Omega}) \rangle (1 + a)]. \quad (7)$$

The relaxation time is given by²¹

$$T_{1n}/T_{1s} = (k_B T)^{-1} \int_{-\infty}^{\infty} d\omega f(\omega) [1 - f(\omega)] \times [n^2(T, \omega) + \bar{n}^2(T, \omega)], \quad (8)$$

where

$$n(T, \omega) = \left\langle \text{Re} \frac{\omega}{[\omega^2 - \Delta^2(T, \vec{\Omega})]^{1/2}} \right\rangle$$

and

$$\bar{n}(T, \omega) = \left\langle \text{Re} \frac{\Delta(T, \vec{\Omega})}{[\omega^2 - \Delta^2(T, \vec{\Omega})]^{1/2}} \right\rangle. \quad (9)$$

In Eq. (3), $n(\omega_i) n(\omega_f) C(\omega_i, \omega_f) \cong n^2(\omega) + \bar{n}^2(\omega)$. The results for T_{1s} are generally insensitive to the precise form of $P(a)$.^{6, 22} For the present calculations a rectangular shape of height $1/(2a_0)$ and width $2a_0$ was used. The normalization of $P(a)$ yields $a_0 = (3\langle a^2 \rangle)^{1/2}$, where $\langle a^2 \rangle$ is the mean-square anisotropy. For pure anisotropic superconductors the relaxation times have been calculated numerically as a function of $\langle a^2 \rangle$ and $\alpha = 2\Delta_0(0)/k_B T_c$.

The effects of nonmagnetic impurities on energy-gap anisotropy have also been calculated by Clem.²³ The results illustrate Anderson's theorem¹¹ on dirty superconductors which, in effect, says that as the mean free path is reduced below the coherence length, crystal momentum is no longer a constant of the motion for quasiparticle states. In-

stead the correct quasiparticle states are exact time-reversed states which, due to the impurity scattering, contain momentum values taken from the entire Fermi surface. The quasiparticles in the dirty superconductor have only a partial memory of the anisotropy due to a particular crystal momentum, and the net result is an averaging out of the effects of gap anisotropy. As the mean free path is reduced the broadening of the density of states is also reduced, and an average BCS-like density of states is recovered in the impure limit.

B. Quasiparticle Damping

The minimum energy of the excited quasiparticles in a BCS superconductor occurs at the gap edge $\omega = \Delta_0(T)$. Just above this gap edge the density of quasiparticle excitations is very large, and it is these low-lying excitations which play the most important role in SLR. At finite temperatures the quasiparticle states have a finite lifetime due to scattering by thermal phonons. A quasiparticle can be scattered into another state with emission or absorption of a phonon, or two excited quasiparticles can annihilate with the emission of a phonon to form a superconducting ground-state pair.²⁴ The quasiparticle lifetime due to these processes depends both on the thermal population of the phonon states and on the dynamic electron-phonon coupling strength.

Both of these processes give rise to an imaginary part of the energy gap at the gap edge which smears the density of states. We define a complex energy-dependent gap,

$$\begin{aligned} \Delta(T, \omega, \delta) &= \Delta_1(T, \omega) + i\Delta_2(T, \omega) \\ &= \Delta_0(T, \omega) [1 + i\delta(T, \omega)], \end{aligned} \quad (10)$$

where $\Delta_0(T, \omega)$ is the BCS gap parameter, and $\delta(T, \omega) = \Delta_2(T, \omega)/\Delta_0(T, \omega)$. We further assume that the energy gap is essentially independent of energy at small energies $\Delta_0(T, \omega) \ll \omega_D$, i. e.,

$$\Delta(T, \omega) = \Delta[T, \omega = \Delta_0(T)], \quad (11)$$

and subsequently drop the energy argument.

The change in the BCS density of states due to quasiparticle damping alone is evaluated from the expression

$$n(\omega, \delta) = \text{Re} \frac{\omega}{[\omega^2 - \Delta_0^2(T)(1 + i\delta)^2]^{1/2}}, \quad (12)$$

with a similar expression for $\bar{n}(\omega, \delta)$:

$$\bar{n}(\omega, \delta) = \text{Re} \frac{\Delta_0(T)(1 + i\delta)}{[\omega^2 - \Delta_0^2(T)(1 + i\delta)^2]^{1/2}}. \quad (13)$$

The imaginary part of the energy gap has been calculated by both Fibich¹² and Scalapino and Wu.²⁴ The latter calculation has been extended to the higher-temperature range $T/T_c \leq 0.9$ and is given

by²⁵

$$|\delta| = \frac{|\Delta_2(T)|}{\Delta_0(T)} = \frac{n\pi\lambda}{1+\lambda} \left(\frac{T}{\Theta_D}\right)^n \left[\Gamma\left(\nu + \frac{3}{2}\right) \zeta\left(\nu + \frac{3}{2}\right) \times \left(\frac{k_B T}{2\Delta_0(T)}\right)^{3/2} + \frac{\pi^{1/2}}{n} \left(\frac{2\Delta_0(T)}{k_B T}\right)^{3/2} e^{-\Delta_0(T)/k_B T} \right]. \quad (14)$$

Here Γ and ζ are the Γ and Riemann ζ functions, respectively, Θ_D is the Debye temperature, and λ is the dimensionless electron-phonon coupling constant. At low frequencies the effective electron-phonon coupling strength $\alpha^2(\omega)$ times the phonon frequency distribution $F(\omega)$ varies as ω^n . For "jellium,"²⁴ $n=2$; although umklapp processes may modify this behavior and lead to $n=1$, we find that for reasonable values of T_c , Θ_D , and λ , $n=1$ yields too large a gap broadening to fit our experimental results. Therefore we have used Eq. (14) with $n=2$ in the treatments of QPD effects on $T_1(T)$ discussed below.

C. Superposition of EGA and QPD

In pure indium, EGA is expected to play a dominant role in determining the structure of the density of states at the gap edge and hence the observed $T_1(T)$. In addition, quasiparticle damping effects should also contribute to the density-of-states structure at the gap edge. Unfortunately no microscopic theory which simultaneously includes these mechanisms has been reported.

In the approximation that these effects are independent of each other we have formulated a combined model which includes both mechanisms. The effect of each mechanism separately is the introduction of structure into the energy-gap parameter which we now write as $\Delta(T, a, \delta)$. We consider an energy-gap parameter which includes each of these mechanisms as

$$\Delta(T, a, \delta) = \langle \Delta(T, \delta) \rangle (1 + a), \quad (15)$$

where

$$\langle \Delta(T, \delta) \rangle = \Delta_0(T) (1 + i\delta) \quad (16)$$

contains the strong coupling features. In essence we assume that the quasiparticle damping is isotropic. The effective density of states is then

$$n(\omega, a, \delta) = \text{Re} \left\langle \frac{\omega}{[\omega^2 - \Delta^2(T, a, \delta)]^{1/2}} \right\rangle. \quad (17)$$

A similar calculation is made for $\bar{n}(\omega, a, \delta)$.

D. Energy-Gap Inhomogeneity; Additional Residual Broadening

Inhomogeneities of the effective interaction between electrons will cause a significant deviation from the BCS-type relaxation time only if the characteristic size r_c of the inhomogeneities is smaller than the pair dimension ξ_0 . Suppose $r_c \gg \xi_0$: Then those quasiparticles which relax a given nucleus

will have a local BCS character, and the relaxation time will be small, i. e., the relaxation rate will be large. The relaxation rate of the entire sample is just an average of such large rates, so that the measured relaxation rate will be nearly the BCS result.

On the other hand, if $r_c \ll \xi_0$, those quasiparticles which relax a given nucleus will sample several inhomogeneities and hence will have a smeared BCS distribution, dependent on a spatial average of the effective interaction over a volume of dimension $\approx \xi_0^3$. The result will be a temperature-independent relative gap broadening, whose effect is similar to gap anisotropy. Indeed, the phenomenological model of EGA can be used to describe this sort of gap inhomogeneity. We merely rewrite $\langle a^2 \rangle$ as $\langle \mu^2 \rangle$, and interpret $\langle \mu^2 \rangle$ as a mean-squared relative gap broadening due to inhomogeneities.

It is clear that EGI is not a unique candidate for any observed temperature-independent residual broadening, although to the authors's knowledge no plausible alternative mechanism has been suggested.

IV. EXPERIMENTAL RESULTS

A. Pure Indium

Figure 3 shows our experimental results for $T_1(T)$ in pure indium. The solid curve represents the best fit to the data using both the EGA theory alone, and also the combined EGA + QPD model discussed in Sec. III. Within errors, the parameters obtained for the EGA contribution $\langle a^2 \rangle = 0.005 \pm 0.001$, $\alpha = 3.50 \pm 0.10$ are the same in both cases.²⁶ The values of $\Theta_D = 111$ K and $\lambda = 0.75$ were not varied. Also within errors, the above value of $\langle a^2 \rangle$ and α are insensitive to the presence of the small residual broadening observed in the dirty alloys (see Sec. IV B). The model independence of $\langle a^2 \rangle$ and α indicates the EGA is the dominant broadening mechanism in pure indium, and lends confidence to the numerical values of $\langle a^2 \rangle$ and α quoted above.

B. Alloys

Within experimental error, the measurements of $T_1(T)$ for all alloy systems were dependent only on the residual resistivity ratio $\rho = R_{4.2\text{K}} / (R_{273\text{K}} - R_{4.2\text{K}})$ and were independent of solute species. The $T_1(T)$ curves can be characterized by (i) the low-temperature slope B , and (ii) the minimum value of $T_1(T)$, $T_{1\text{min}}$, which occurs near $T_c/T \approx 1.1$. In the range $1.4 < T_c/T < 2.5$, the data were fit to a straight line of the form

$$\ln(T_1) = A + B(T_c/T) \quad (18)$$

by the least-squares method. The slope is not a direct measure of the energy gap since the extreme low-temperature regime was not attained in the present work; it is used only to summarize the

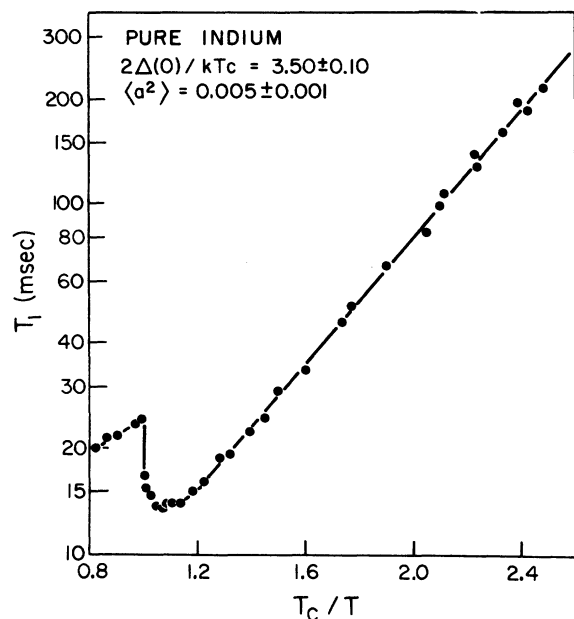


FIG. 3. $T_1(T)$ in pure indium. The solid curve is the result of the EGA theory of Clem (Ref. 21) and also of the combined EGA+QPD model described in the text.

measurements in the alloys at moderately low temperatures. These are essentially independent of solute kind and concentration, as shown in Fig. 4. The average value of B is 2.02 ± 0.10 .

The value of $T_{1\text{min}}/T_{1n}$ reflects the broadening of the BCS density of states: it is shown in Fig. 5 for In-based (this work) and Al-based alloys¹⁰ as a function of the dimensionless parameter $\eta = (2\Delta_0 \times \tau \langle a^2 \rangle)^{-1}$, where τ is the mean impurity-scattering

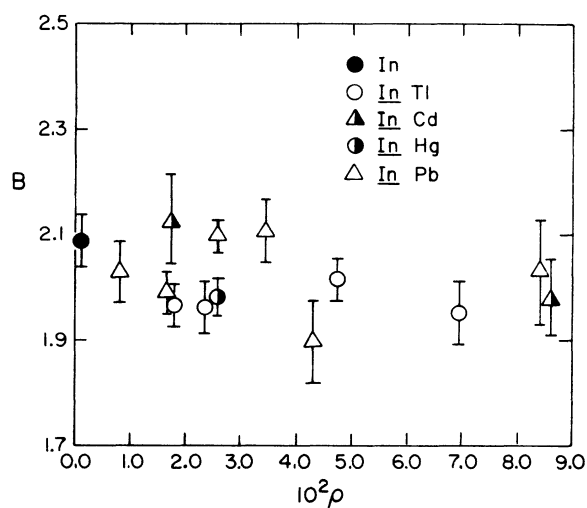


FIG. 4. Dependence of the experimental slope $B = d[\ln(T_1)]/d(T_c/T)$ on the residual resistance ratio ρ .

time. The quantity η is proportional to the impurity concentration and inversely proportional to the mean free path l . In the impure limit, $T_{1\text{min}}/T_{1n}$ should be a universal function of η (shown by the solid curve in Fig. 5) according to the theory of Clem.²³ Uncertainty in the measured ratio of conductivity to mean free path (of about a factor of 2 in indium²⁷) leads to the same uncertainty in η . Our conclusions, however, will not be appreciably affected.

Although there is a discrepancy between the measured values of $T_{1\text{min}}/T_{1n}$ and the EGA theory for the alloys, the initial decrease of $T_{1\text{min}}/T_{1n}$ with concentration indicates that EGA is an important broadening mechanism in pure In and Al. The discrepancy at the larger concentrations can be explained by the presence of additional impurity-independent broadening mechanisms which are relatively unimportant compared to EGA in pure indium, but which dominate as EGA is averaged out. Such mechanisms are quasiparticle damping and energy-gap inhomogeneity.

The situation in the impure limit in the indium alloys has been discussed previously.¹⁵ An acceptable fit to the data was obtained using a combined EGI and QPD model formulated in analogy with the EGA+QPD model of Sec. III C above. The values of Θ_D and λ were taken to be 111 K and 0.75, respectively, while α and the mean-square inhomogeneity $\langle \mu^2 \rangle$ were varied for best fit. The parameters

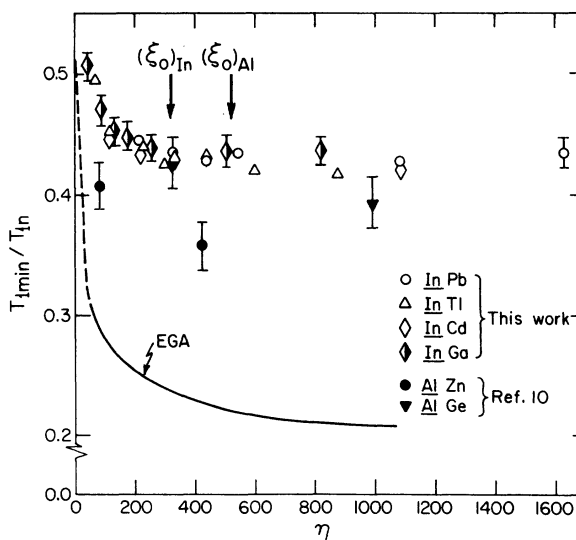


FIG. 5. Dependence of $T_{1\text{min}}/T_{1n}$ on the dimensionless parameter $\eta = (2\Delta_0 \tau \langle a^2 \rangle)^{-1}$, for indium- and aluminum-based alloys. Here τ is the mean impurity-scattering time. The values of η which correspond to mean free paths equal to the BCS coherence length ξ_0 are indicated for the two systems. The curve labeled "EGA" gives the results of Ref. 23 for the reduction of EGA by impurity scattering.

obtained are $\alpha = 3.50 \pm 0.10$ and $\langle \mu^2 \rangle = 0.0005 \pm 0.00005$, which represents a residual temperature- and impurity-independent relative gap broadening of about 2% rms. In aluminum the electron-phonon interaction is relatively weak, and we believe that the residual broadening in this case is essentially entirely due to EGI of about half the rms value in indium.

V. DISCUSSION

A. Pure Indium and Aluminum

Gap anisotropy appears to be the dominant density-of-states broadening mechanism in pure indium. This conclusion is supported by the observed reduction of $T_1(T)$ as the mean free path is shortened to the point at which gap anisotropy is averaged out. Similar behavior of $T_1(T)$ is observed in aluminum. Within experimental error we conclude that gap anisotropy is averaged out when the mean free path $l < \xi_0$, consistent with the Anderson theory.¹¹

The experimental mean-square anisotropy obtained in the Clem model, $\langle a^2 \rangle = 0.005 \pm 0.001$ for pure indium, is insensitive either to the presence of quasiparticle damping or to the observed residual broadening in the dirty alloys, as discussed in Sec. IV. For pure aluminum we find $\langle a^2 \rangle = 0.003 \pm 0.001$ when a similar fit is made to the data of Masuda and Redfield.⁴ (See note added in proof.)

The value of the anisotropy we derive in this work for indium is smaller than the value of $\langle a^2 \rangle = 0.021$ obtained by the Markowitz and Kadanoff (MK) analysis²⁸ of the transition temperature dependence on mean free path. T_c measurements in *InTl* alloys by Gubser *et al.*²⁹ yielded $\langle a^2 \rangle = 0.0185$, also using the MK analysis. However, the MK model as employed by these authors only determines the product $\lambda_c \langle a^2 \rangle$, where λ_c is the ratio of the mean collision times for transport processes and for smoothing out of EGA. Carriker and Reynolds²⁷ (CR) extended the MK work and were able to determine λ_c and $\langle a^2 \rangle$ separately from T_c measurements on *InPb* alloys. They found $\langle a^2 \rangle = 0.0072 \pm 0.0007$ and $\lambda_c > 3$. CR also used the predictions of Clem³⁰ to extract an independent value of $\langle a^2 \rangle = 0.007$ from critical-field-curve measurements. These values are in substantial agreement with our results.

B. Alloys

Although the gap-anisotropy-broadening effects are apparently averaged out in the more concentrated alloys, $T_1(T)$ is still larger than predicted by the unmodified BCS theory. This suggests that additional impurity-independent broadening mechanisms exist in the alloys. Quasiparticle damping is expected to account for at least part of the residual

broadening,⁶ but calculations of the temperature dependence of T_1 from the QPD theory show that in both aluminum and indium this mechanism is not strong enough to account for the observed T_1 behavior.¹⁵ In particular, the low-temperature slope B of Sec. IV B should be considerably reduced in the alloys if QPD dominates, contrary to the data shown in Fig. 4.

An additional temperature- and impurity-independent relative gap broadening is necessary to fit the data. In the absence of an alternative mechanism, we believe this is evidence of a 2% rms distribution of the effective electron-phonon interaction within the sample. Because the relaxation times differ from those expected in the presence of local BCS behavior, we conclude that the scale of the inhomogeneities r_c is smaller than ξ_0 . We fix the lower limit on r_c as approximately 100 Å since, if $r_c < 100$ Å, Bergmann³¹ has shown that the ratio $2\Delta_0/k_B T_c$ increases to values larger than our observed value of 3.50. No simple method for the determination of r_c has been found to date.

As described in a preliminary report,¹⁵ equally good fits to the *In* alloy data can be made using either the EGI+QPD model discussed above or an "EGI only" model, i.e., the assumption that QPD plays no role at all is qualitatively consistent with our results. Evidence for the inapplicability of this latter picture is obtained from the values of the parameter $\alpha = 2\Delta_0(0)/k_B T_c$ obtained from the fits. For the "EGI only" fit α was found to be $(6 \pm 3)\%$ less than for pure indium, whereas for the EGI+QPD fit the difference was $(0 \pm 3)\%$. To our knowledge there is no independent evidence for a decrease of α with solute concentration, so that the EGI+QPD picture appears to be correct. The considerable experimental evidence for the reality of QPD effects would in any case make a single contrary result suspect. Nevertheless our data are not accurate enough to permit determination of the parameters involved in the QPD theory, and we do not claim to have obtained a clear observation of QPD in indium alloys.

VI. CONCLUSION

The distribution and damping of excited quasiparticle states in superconducting indium-based alloys have been studied by nuclear spin-lattice relaxation measurements. There are three energy-gap broadening mechanisms which determine the superconducting density of states. Energy-gap anisotropy accounts for the distribution of gaps in indium and very dilute alloys of indium. Impurity scattering in the alloys averages out EGA effects, and the distribution of energy gaps is independent of anisotropy when the mean free path is less than dimension ξ_0 .

The effect of finite quasiparticle lifetime is un-

observably small compared with that due to EGA in pure indium. In the alloy systems, quasiparticle damping is apparently present but weak. Gap inhomogeneity (or some other residual broadening) of about 2% rms, independent of temperature, solute concentration, and sample species, appear to determine the distribution of the density of states at low temperatures. EGI also appears to play a role in concentrated aluminum-based alloys.

Note added in proof. Wells *et al.* [Phys. Rev. B **1**, 3636 (1970)] have reported observation of a $\sim 6\%$ anisotropy between [100] and [111] directions

by tunneling measurements on single-crystal Al. Although these authors suspect some anisotropy reduction by boundary scattering, their results are consistent with our value of $a_{\text{rms}} = 0.055$. We are grateful to Dr. Wells for bringing this work to our attention.

ACKNOWLEDGMENTS

The authors wish to acknowledge useful discussions with M. Daugherty, R. R. Hewitt, D. N. Langenberg, and E. Šimánek, and to thank Professor Hewitt for the loan of the samples used in this work.

*Work supported by the National Science Foundation.

¹Present address: Argonne National Laboratory, Argonne, Ill. 60439. From a thesis submitted by J. D. Williamson in partial fulfillment of the requirements for the degree of Doctor of Philosophy, University of California, Riverside, Calif.

²J. Bardeen, L. N. Cooper, and J. R. Schrieffer, Phys. Rev. **108**, 1175 (1957).

³L. C. Hebel and C. P. Slichter, Phys. Rev. **113**, 1504 (1959).

⁴A. G. Redfield, Phys. Rev. Lett. **3**, 85 (1959).

⁵Y. Masuda and A. G. Redfield, Phys. Rev. **125**, 159 (1962).

⁶Y. Masuda, IBM J. Res. Dev. **6**, 24 (1962).

⁷J. Butterworth and D. E. MacLaughlin, Phys. Rev. Lett. **20**, 265 (1968).

⁸N. V. Zavaritskii, Zh. Eksp. Teor. Fiz. **43**, 1123 (1962) [Sov. Phys.-JETP **16**, 793 (1963)].

⁹C. K. Campbell and D. G. Walmsley, Can. J. Phys. **45**, 159 (1967).

¹⁰D. M. Ginsberg and L. C. Hebel, in *Superconductivity*, edited by R. D. Parks (Marcel Dekker, New York, 1969), Vol. 1, Chap. 4, pp. 225, 229, and 251.

¹¹Y. Masuda, Phys. Rev. **126**, 1271 (1962).

¹²P. W. Anderson, J. Phys. Chem. Solids **11**, 26 (1959).

¹³M. Fibich, Phys. Rev. Lett. **14**, 561 (1965); Phys. Rev. Lett. **14**, 621 (1965).

¹⁴G. M. Eliashberg, Zh. Eksp. Teor. Fiz. **38**, 966 (1960) [Sov. Phys.-JETP **11**, 696 (1960)].

¹⁵A. I. Larkin and Yu. N. Ovchinnikov, Zh. Eksp. Teor. Fiz. **61**, 2147 (1971) [Sov. Phys.-JETP **34**, 1144 (1972)].

¹⁶J. D. Williamson and D. E. MacLaughlin, in Proceedings of

the Thirteenth International Conference on Low Temperature Physics, Boulder, Colo., 1972 (unpublished).

¹⁷W. T. Anderson, F. C. Thatcher, and R. R. Hewitt, Phys. Rev. **171**, 541 (1968).

¹⁸F. C. Thatcher and R. R. Hewitt, Phys. Rev. B **1**, 454 (1970).

¹⁹J. D. Williamson and D. E. MacLaughlin, Phys. Rev. B **5**, 2738 (1972).

²⁰D. E. MacLaughlin, J. D. Williamson, and J. Butterworth, Phys. Rev. B **4**, 60 (1971).

²¹D. E. MacLaughlin and J. Butterworth, Phys. Lett. **23**, 291 (1966).

²²J. R. Clem, Ann. Phys. (N.Y.) **40**, 268 (1966).

²³J. P. Carbotte and P. T. Traunt, Can. J. Phys. **50**, 563 (1972).

²⁴J. R. Clem, Phys. Rev. **148**, 392 (1966).

²⁵D. J. Scalapino and T. M. Wu, Phys. Rev. Lett. **17**, 315 (1966).

²⁶D. J. Scalapino and B. N. Taylor (unpublished).

²⁷The value of $\langle a^2 \rangle = 0.020$ given in Ref. 6 was in error, due to an inadequate approximation in the numerical integration required for the fit.

²⁸R. C. Carriker and C. A. Reynolds, Phys. Rev. B **2**, 3991 (1970).

²⁹D. Markowitz and L. P. Kadanoff, Phys. Rev. **131**, 563 (1963).

³⁰D. U. Gubser, D. E. Mapother, and D. L. Connelly, Phys. Rev. B **2**, 2547 (1970).

³¹J. R. Clem, Phys. Rev. **153**, 449 (1967).

³²G. Bergmann, Z. Phys. **228**, 25 (1969).

Theory of Photon-Assisted Tunneling in Superconducting Junctions with Active Barrier Impurities

Richard D. Sherman

Physics Department, University of Illinois, Urbana, Illinois 61801

(Received 8 December 1972)

A model is proposed to theoretically study photon-assisted tunneling in superconducting junctions with active molecular impurities in the barrier. A simple calculation is performed to demonstrate the method. Temperature Green's functions are employed so that it is possible to include known results on strong coupling superconductors while extending theory to include molecular-impurity effects.

Our understanding of tunneling phenomena has advanced considerably since Bardeen¹ realized how a metal-insulator-metal sandwich could be treated

as two bulk metals weakly coupled, by introducing a phenomenological Hamiltonian. This has allowed us to use tunneling as a probe of metallic band struc-